

<https://doi.org/10.15407/ujpe68.11.764>

V.O. YUKHYMCHUK,<sup>1</sup> V.M. DZHAGAN,<sup>1</sup> O.F. ISAIEVA,<sup>1</sup> P.M. LYTVYN,<sup>1</sup>  
A.A. KORCHOVYI,<sup>1</sup> T.M. SABOV,<sup>1</sup> V.B. LOZINSKII,<sup>1</sup> V.S. YEFANOV,<sup>1</sup>  
V.O. OSOKIN,<sup>2</sup> YU.A. KURAPOV<sup>2</sup>

<sup>1</sup> V.Ye. Lashkaryov Institute of Semiconductor Physics, Nat. Acad. of Sci. of Ukraine  
(45, Nauky Ave., Kyiv 03028, Ukraine)

<sup>2</sup> Ye.O. Paton Electric Welding Institute, Nat. Acad. of Sci. of Ukraine  
(11, Kazymira Malevycha Str., 03150 Kyiv, Ukraine)

## STRUCTURAL AND MORPHOLOGICAL PROPERTIES OF NANOMETER CARBON FILMS OBTAINED BY ELECTRON BEAM SPUTTERING OF GRAPHITE

---

*Nanometer-thick carbon films on metal (copper, steel) and silicon substrates are obtained by the electron sputtering of graphite. The substrate temperature was varied from 350 to 600 °C with an increment of 50 °C, and the sputtering time from 1 to 10 s. The produced carbon films are studied using Raman spectroscopy, X-ray photoelectron spectroscopy (XPS), atomic force microscopy, and electron paramagnetic resonance (EPR) spectroscopy. From the analysis of Raman spectra, it is found that, at the temperatures of metal substrates below 550 °C, the carbon films formed on them are amorphous and have a graphite-like structure at higher substrate temperatures. At the same time, the films formed on silicon substrates at temperatures below 600 °C are amorphous. The results obtained from the Raman spectra correlate with the XPS data. It is shown that both the temperature and the substrate material (metal or silicon) affect the film morphology. As the substrate temperature increases from 350 to 600 °C, the average size of surface irregularities increases for carbon films on both the metal and silicon substrates. The EPR studies show that the available structural film defects, which are responsible for the manifestation of the so-called defect bands (D and D' ones) in the Raman spectra, are not paramagnetic.*

*Keywords:* AFM, carbon amorphous films, electron sputtering, graphite-like films, Raman spectroscopy, XPS.

---

Citation: Yukhymchuk V.O., Dzhagan V.M., Isaieva O.F., Lytvyn P.M., Korchovyi A.A., Sabov T.M., Lozinskii V.B., Yefanov V.S., Osokin V.O., Kurapov Yu.A. Structural and morphological properties of nanometer carbon films obtained by electron beam sputtering of graphite. *Ukr. J. Phys.* **68**, No. 11, 764 (2023). <https://doi.org/10.15407/ujpe68.11.764>.

Цитування: Юхимчук В.О., Джаган В.М., Ісаєва О.Ф., Литвин П.М., Корчовий А.А., Сабов Т.М., Лозінський В.Б., Єфанов В.С., Осокін В.О., Курапов Ю.А. Структурні та морфологічні властивості нанометрових вуглецевих плівок, отриманих розпиленням графіту електронним променем. *Укр. фіз. журн.* **68**, № 11, 766 (2023).

### 1. Introduction

Interest in the research of various types of carbon materials permanently grows [1–5]. This occurs due to their wide application in electrocatalysis, electrosynthesis, and graphene nanoelectronics, as well as when creating protective coatings and giving special properties to base materials, when carbon films are deposited on them; in particular, this concerns the anti-reflection coating of solar cells, the creation of a superhard or/and heat-resistant surface

shell, and so forth [1–7]. Nowadays, challenging remains the issue of producing thin (nanometers) carbon films with predetermined properties on various substrates. Depending on the deposition methods, as well as the technological parameters and characteristics of substrates, carbon films with various structures can be formed, e.g., films with amorphous carbon [8], graphite films [9], and films with a high content of carbon atoms with  $sp^3$ -bonds, the so-called diamond-like films (DLFs) [10]. The latter are intensively used for coating various materials, because they are characterized by a combination of such physicochemical properties as the high hardness, wear resistance, chemical inertness, wide band gap, low friction coefficient, biocompatibility, and so on [11, 12].

After the discovery of graphene [13], the interest in obtaining carbon films with  $sp^2$ -bonds has increased substantially because, by varying the number of carbon layers, it is possible to obtain both single- and multilayer graphene films, which are characterized by properties important for applications. As is known, graphene is a two-dimensional layer composed of benzene rings. It attracts high attention due to its specific and unusual properties, in particular, the quantum electron transport, a tunable band gap, an extremely high charge carrier mobility, and others [13].

All the above forms a basis for the creation of new technologies or the improvement of available ones for producing carbon films with predetermined properties. The purpose of this work is to find how the technological parameters of the electron beam sputtering of high-purity graphite and the substrate parameters affect the structural and morphological properties of ultrathin (nanometers) carbon films.

## 2. Experimental Technique

An electron beam installation UE-142 was used to deposit carbon films on substrates. The process of graphite sputtering followed by the carbon film deposition is schematically shown in Fig. 1.

A high-purity graphite rod with a tungsten washer on its upper end was arranged in a water-cooled copper crucible. The electron beam heated tungsten to the melting temperature ( $\approx 3422$  °C). At this temperature, carbon atoms and clusters evaporated from the graphite and, when passing through the molten tungsten layer, were separated by size. As was shown

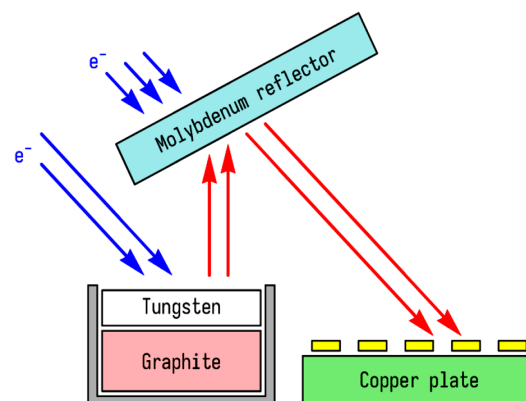


**Fig. 1.** Schematic diagram describing the production of carbon films on substrates of various types

in work [14], the flow of carbon vapor that passed through the tungsten bath consisted of nanoclusters with dimensions of about 1–2 nm.

The next factor that affected the parameters of the carbon vapor flow was a molybdenum reflector heated to the temperature  $T_{cr} \approx 1696$  °C. When interacting with the heated reflector surface, carbon nanoclusters either can play the role of the formation centers of a carbon coating on it (at the reflector temperatures lower than  $T_{cr}$ ), or they can be reflected from its surface (at temperatures higher than  $T_{cr}$ ). By changing the inclination angle of the reflector heated above  $T_{cr}$ , it is possible to control the carbon flux and condense it on substrates of various types. As the latter, copper, steel, and silicon plates were used, whose temperature was varied from 350 to 600 °C with an increment of 50 °C. The substrates were arranged on a copper plate, which was heated by the electric current or cooled by running water to maintain the required temperature. The vacuum level in the technological chamber was  $1.33 \times 10^{-2}$  Pa, the electron beam current in the tungsten bath was  $I_c = 0.42$  A, the electron acceleration voltage was  $U = 20.0$  kV, and the duration of the film sputtering process was varied from 1 to 10 s.

The deposited carbon films were studied with the help of Raman spectroscopy, X-ray photoelectron spectroscopy (XPS), atomic force microscopy (AFM), and electron paramagnetic resonance (EPR) methods. The Raman spectra were excited using the radiation emission from a solid-state laser with a wavelength of 457 nm, and they were registered on an MDR-23 single-stage spectrometer (LOMO)

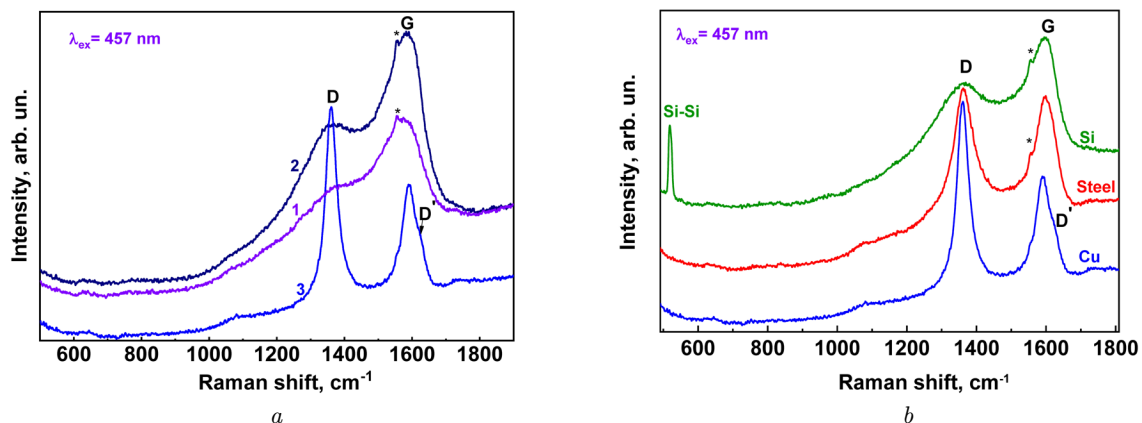


**Fig. 2.** Raman spectra of carbon films: formed on copper substrates at deposition temperatures of 350 (1), 385 (2), and 550 °C (3); and formed on copper, steel, and silicon substrates at a deposition temperature of 550 °C (b). The deposition time was 10 s for all films. Asterisks (\*) mark the band induced by the scattering of a non-fundamental lasing mode

equipped with a cooled CCD detector (Andor iDus 420, UK). In order to prevent heat-induced modifications of the specimens during their research, the power density of laser radiation at the specimens was maintained lower than  $10^3 \text{ W/cm}^2$ . The spectral resolution of the spectrometer was determined by the width of the phonon band from the silicon monocrystalline substrate and was evaluated to equal  $3 \text{ cm}^{-1}$ . The frequency position of the phonon band from Si ( $521.0 \text{ cm}^{-1}$ ) was used as a reference to determine the frequency positions of other Raman bands.

The surface morphology of the films was studied on the Atomic Force Microscope NanoScope IIIa (Digital Instruments) in the Tapping Mode. Before and after the measurements, the probes were tested to control the tip shape. The measurements were made using the probes with a high symmetry degree, and whose cross-section radius at a distance of 10 nm from the tip did not exceed 6 nm.

The XPS analysis was performed on a PHI 5600 LS spectrometer using a monochromatic Al K(alpha)

**Elemental composition of films**

Specimen	C, at.%	O, at.%	N, at.%	Cu, at.%	Mo, at.%	Si, at.%
Carbon film, 550 °C, on Cu	91.95	6.6	0.18	0.14	0.26	0.88
Carbon film, 350 °C, on Cu	92.94	6.74	–	0.18	0.14	–

X-ray source. The peak positions were adjusted in accordance with the metal gold peak Au 4f 7/2 ( $E_b = 84 \text{ eV}$ ), and the scale linearity was adjusted according to the positions of the peaks Au 4f 7/2 ( $E_b = 84 \text{ eV}$ ) and Cu 2p 3/2 ( $E_b = 932.6 \text{ eV}$ ). The review spectra were registered with an energy window of 93.9 eV and with an increment of 0.4 eV in an energy interval of 0–1400 eV.

The determined elemental composition of the films is quoted in Table. Note that the total percentage of elements can differ from 100% because of the data rounding made by the applied software.

**3. Results and Their Discussion**

In Fig. 2, a, the Raman spectra of the carbon films formed on copper substrates are depicted. One can see that the spectra of the films formed at temperatures below 550 °C (curves 1 and 2) correspond to that of a structure typical of amorphous, highly defective or tetrahedrally coordinated (with a high content of the  $sp^3$ -phase) carbon films [15, 16], whereas the spectrum of the film formed at 550 °C (curve 3) corresponds to the spectrum of a graphite-like structure with the predominating bonds of the  $sp^2$ -type [15, 16].

Figure 2, b exhibits the Raman spectra of the carbon films formed on copper, steel, and silicon substrates at a temperature of 550 °C. The figure makes it evident that not only the temperature, but also the substrate material affect the structure of carbon films. Really, the spectra of the films formed on copper and steel substrates are quite similar and typical

of a graphite-like structure, whereas the spectrum of the film formed on a Si substrate is typical of an amorphous carbon structure. It seems that one of the important substrate parameters affecting the film structure is the thermal conductivity of the film.

In Fig. 3, the Raman spectra of the carbon films formed on copper (1) and Si (2) substrates at a temperature of 550 °C and on a copper substrate at a temperature of 350 °C (3) are shown in the interval of vibrational modes of the first and second orders. One can see that the second-order bands 2G, D + G, 2D, and D + T clearly manifest themselves only in the spectrum of the carbon film formed on a copper substrate at 550 °C. This fact testifies to the formation of a carbon film with a predominant content of the  $sp^2$ -phase (a graphite-like structure). At the same time, it is worth noting that the carbon film contains structural defects in this case as well, which is evidenced by a high intensity of D-band.

Note also that the aforementioned defects are not paramagnetic centers, which was evidenced by radio spectroscopic studies of all those films. As a rule, during the carbon film deposition, nanoclusters nucleate first. As time goes, depending on the technological conditions of the film growing, they can overlap due to the increase of either their size or their number to form a continuous film.

The number of defects observed in carbon films depends on many factors, including the size of formed carbon nanoclusters. Indeed, the films with a graphite-like structure can contain defects of various types. In particular, these are the Stone–Wales defect (the substitution of benzene rings in graphene layers by two “pentagon + heptagon” pairs), the defect “vacancy + atom with a broken C–C bond”, and nanocluster boundaries, which can also be considered as defects [17].

To estimate the size of the formed carbon nanoclusters, the Raman spectra were resolved into separate components described by the Gaussian or Lorentzian functions, as is shown in Fig. 4. In all cases, the Raman spectra were resolved into five separate bands [18]:

1) the band corresponding to the vibrations of oleic chains;

2) band *D* corresponding to the “breathing” modes of benzene rings, with defects in the graphite crystalline structure at points *K* and *K'* of the Brillouin zone mandatory participating in this process;

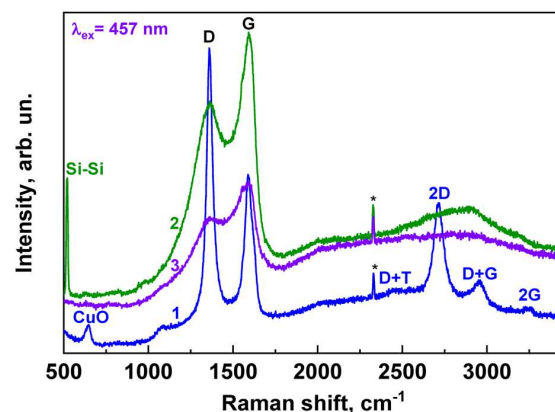


**Fig. 3.** Raman spectra of carbon films formed on copper (1) and Si (2) substrates at a temperature of 550 °C, and on a copper substrate at a temperature of 350 °C (3); the spectra were measured in the spectral interval of the first- and second-order vibrational modes

3) the band corresponding to amorphous carbon; the latter may consist of disordered chains and clusters with  $sp^3$ -,  $sp^2$ -, and  $sp^1$ -bonds;

4) band *G* corresponding to the stretching vibrations of the pairs of carbon atoms; this mode corresponds to the center of the Brillouin zone and, unlike the *D*-band, does not require the mandatory presence of benzene rings in the structure;

5) band *D'* corresponding to vibrational modes that, similarly to the *D*-band case, appear only in the presence of film defects taking part in the scattering to “provide” the preservation of the total momentum sum during the Raman scattering process; however, unlike band *D*, band *D'* is activated by the intra-valley scattering process [17].

Using the results of the spectral resolution (Fig. 4), the integral intensities of the bands *D* and *G* were determined. Later, they were used to evaluate the average sizes of carbon nanocrystals according to the formula [19]

$$L_a[\text{nm}] = \frac{560}{E_l^4} \times \left( \frac{I_D}{I_G} \right)^{-1},$$

where  $L_a$  is the average size of nanocrystals in nanometer units,  $E_l$  is the photon energy of the exciting laser radiation (in our case, it is equal to 2.71 eV), and  $I_D/I_G$  is the ratio between the integral intensities of bands *D* and *G*. As a result of calculations, it is found that  $L_a \approx 4.9$  nm for the film formed at 350 °C, and  $L_a \approx 5.6$  nm for the formed at 550 °C. Thus, the

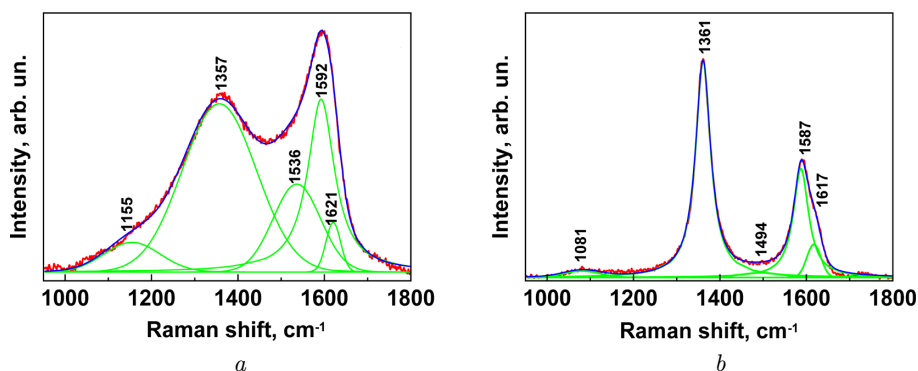


**Fig. 4.** Raman spectra of carbon films formed on copper substrates at temperatures of 350 (a) and 550 °C (b) and their resolution into components

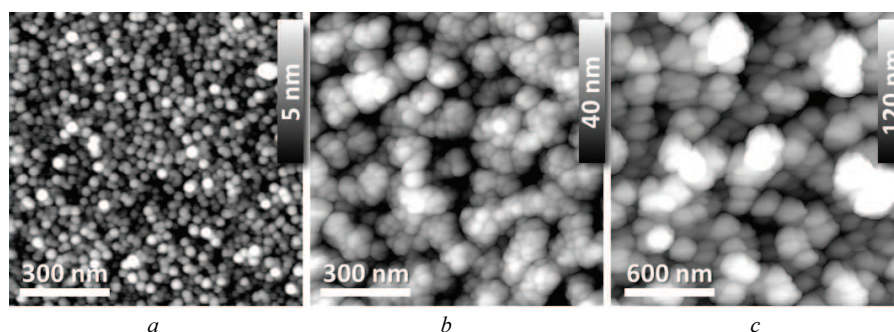


**Fig. 5.** AFM images of the surfaces of carbon films formed on Si substrates at temperatures of 350 (a) and 550 °C (b) and on Cu substrates at a temperature of 500 °C (c). Surface roughness (RMS) in Fig. 5, a, b, c is 1.2, 10.3, and 33.5 nm, respectively

average sizes of carbon clusters did not differ substantially, which was a result of a small difference between the substrate temperatures at which those films were formed.

At the same time, the sizes of the inhomogeneities formed on the surface of the films deposited on Si substrates at 350 and 550 °C (Figs. 5, a and 5, b, respectively) and on a copper substrate at a temperature of 550 °C (Fig. 5, c) differ considerably. As one can see from Fig. 5, the increase of the silicon substrate temperature gave rise in the size of inhomogeneities both in height and in lateral directions. Moreover, the surface morphology of carbon films is also influenced by the parameters of the substrate itself. Under the same technological deposition conditions, grains with larger sizes and different shapes were formed on a copper substrate (Fig. 5, c) as compared with the silicon substrate case (Fig. 5, b).

Hence, besides the substrate temperature, other substrate parameters are important, e.g., its ther-

mal conductivity, the presence of an oxide layer on the substrate surface, the presence of impurities and others. Indeed, a lot of works were devoted to the study of how impurities affect the structure of carbon films. In particular, it was shown that higher iron contents in carbon films change their electrical, electrochemical, and structural properties [20], and the growth of the silicon content brings about structural changes in them [21].

In Table, the elemental compositions of carbon films formed on copper substrates at temperatures of 350 and 550 °C are presented. The presence of oxygen and nitrogen impurity atoms in the films can be a result of their capture by the carbon vapor flow from the residual atmosphere in the installation. As for the available Mo, Si, and Cu impurities, they could be in both the tungsten bath and the molybdenum screen. As was marked above, the Raman spectra of those films differ substantially (see Fig. 4). According to XPS diagnostics, silicon (0.88 at%) and nitrogen



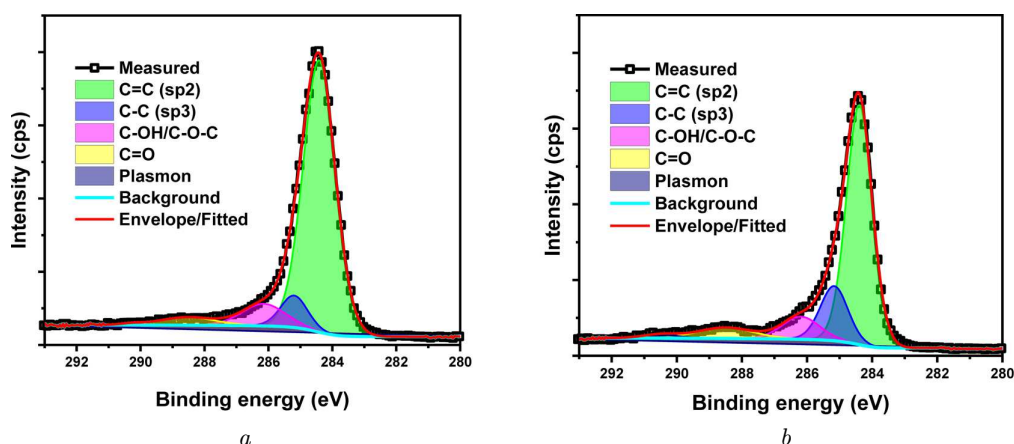


**Fig. 6.** XPS spectra of carbon films formed on copper substrates at temperatures of 550 (a) and 380 °C (b)

(0.18 at%) were contained in the film formed at a higher temperature, but they were absent in the film formed at 350 °C. Although the content of those elements is insignificant, this fact should be taken into account, because the matter concerns nanometer-thick films, and the presence of those elements in carbon films can also affect the formation of their structure. However, in order to draw quantitative conclusions about their impact, the additional research will be performed in the future.

It is well known that if carbon films are excited by laser radiation in the visible spectral interval, the main contribution to Raman scattering spectra is made by structures with  $sp^2$ -bonds [10, 16]. This occurs, because the energy of laser radiation photons must be higher than 5 eV for the effective excitation of structures with  $sp^3$ -bonds. Nevertheless, the influence of the  $sp^2/sp^3$ -bond ratio quantitatively manifests itself indirectly in the Raman spectra excited by radiation in the visible spectral interval via the variation in the frequency positions of  $D$  and  $G$  bands, their half-widths and intensities. For carbon films formed on copper substrates at temperatures of 350 and 550 °C, the Raman spectra shown in Figs. 4, *a* and 4, *b* correspond to amorphous films and graphite-like films, respectively. At the same time, it was important to determine the absolute contents of the phases with  $sp^2$ - and  $sp^3$ -bonds. For this purpose, the XPS characterization of the above-mentioned films was carried out.

The XPS spectra were measured with a high resolution (with an energy window of 11.75 eV and

an increment of 0.05 eV) in the spectral interval of peak C1s. The obtained spectra were resolved into five components:

- 1) the main peak corresponding to the C=C  $sp^2$ -bonds (284.4 eV);
- 2) the peak related to the C-C  $sp^3$ -bonds (285.2 eV);
- 3) the peak corresponding to the C-OH/C-O-C bonds ( $286.2 \pm 0.1$  eV);
- 4) the peak related to the C=O bonds ( $288.5 \pm 0.1$  eV);
- 5) the peak induced by the plasmon excitation ( $\pi - \pi^*$ -satellite,  $290.2 \pm 3$  eV).

The resolution of the main peak was carried out using the Shirley function, described the background of the spectrum, and used Gaussians and Lorentzians to describe the shapes of other peaks. The content of the  $sp^3$ -phase was determined by analyzing the main peak, and it was found to equal 9% for a carbon film formed on a copper substrate at 550 °C (Fig. 6, *a*), and 20% for a carbon film formed on a copper substrate at 350 °C. The obtained XPS results correlate well with the results of Raman studies.

#### 4. Conclusions

In this work, the comprehensive study of nanometer carbon films formed on substrates of various types (copper, steel, silicon) and at various temperatures and time has been carried out. It is found that the most important technological parameter governing the formation of carbon films with a predominant content of the graphite phase is the substrate tem-

perature, which should be equal to or higher than 550 °C. It is shown that the substrate properties also substantially affect the structure of the films. In particular, a temperature of 550 °C is sufficient to form carbon films with the predominant content of the graphitic phase on metal substrates. At lower substrate temperatures, the fraction of the  $sp^3$ -bonds in the films increases, and films with the amorphous phase are formed. It is found that, besides the substrate temperature, an important parameter affecting the film structure is the thermal conductivity of the substrate: films with graphitic structure are formed on substrates with a high thermal conductivity, and carbon films with the predominant content of the amorphous phase are formed on substrates with a lower thermal conductivity (in particular, on silicon substrates).

It is shown that the substrate temperature also substantially influences the film morphology. The temperature growth from 350 to 550 °C makes the lateral dimensions of surface inhomogeneities of carbon films formed on silicon substrates approximately 1.5 times larger. The same tendency with increasing the temperature is observed for films formed on copper substrates, although the absolute values of lateral inhomogeneities in the latter case are shifted toward larger sizes. On the other hand, it is shown that the growth of the substrate temperature from 350 to 550 °C does not substantially increase the average size of nanocrystals (coherence regions). According to the estimates made using Raman spectroscopy, the average size of carbon nanocrystals increases from 4.9 to 5.6 nm.

- J. Khan, S.A. Momin, M. Mariatti. A review on advanced carbon-based thermal interface materials for electronic devices. *Carbon* **168**, 65 (2020).
- J. Vejpravová. Mixed  $sp^2 - sp^3$  nanocarbon materials: A status quo review. *Nanomaterials* **11**, 2469 (2021).
- M. Rouhani, J. Hobley, F. Chau-Nan Hong, Ye.-R. Jeng. In-situ thermal stability analysis of amorphous Si-doped carbon films. *Carbon* **184**, 772 (2021).
- L. Li, D. Zhang, J. Deng, Y. Gou, J. Fang, H. Cui, Y. Zhao, M. Cao. Carbon-based materials for fast charging lithium-ion batteries. *Carbon* **183**, 721 (2021).
- F. Yin, W. Yue, Y. Li, S. Gao, C. Zhang, H. Kan, H. Niu, W. Wang, Y. Guo. Carbon-based nanomaterials for the detection of volatile organic compounds: A review. *Carbon* **180**, 274 (2021).
- V.S. Kiselov, V.O. Yukhymchuk, M.Ya. Valakh, M.P. Tryus, M.A. Skoryk, A.G. Rozhin, S.A. Kulinich, A.E. Belyaev. Biomorphous SiC ceramics prepared from cork oak as precursor. *J. Phys. Chem. Solids* **91**, 145 (2016).
- R. Kumar, S. Sahoo, E. Joanni, R.K. Singh, W.K. Tan, K.K. Kar, A. Matsuda. Recent progress on carbon-based composite materials for microwave electromagnetic interference shielding. *Carbon* **177**, 304 (2021).
- J. Robertson. Amorphous carbon. *Adv. Phys.* **35**, 317 (1986).
- M. Chhowalla, A.C. Ferrari, J. Robertson, G.A.J. Amaratunga. Evolution of  $sp^2$  bonding with deposition temperature in tetrahedral amorphous carbon studied by Raman spectroscopy. *Appl. Phys. Lett.* **76**, 1419 (2000).
- A.C. Ferrari, J. Robertson. Resonant Raman spectroscopy of disordered, amorphous, and diamondlike carbon. *Phys. Rev. B* **64**, 075414 (2001).
- Z. Seker, H. Ozdamar, M. Esen, R. Esen, H. Kavak. The effect of nitrogen incorporation in DLC films deposited by ECR Microwave Plasma CVD. *Appl. Surf. Sci.* **314**, 46 (2014).
- N. Paik. Raman and XPS studies of DLC films prepared by a magnetron sputter-type negative ion source. *Surf. Coat. Technol.* **200**, 2170 (2005).
- K.S. Novoselov, A.K. Geim, S.V. Morozov, D. Jiang, Y. Zhang, S.V. Dubonos, L.V. Grigorieva, A.A. Firsov. Electric field effect in atomically thin carbon films. *Science* **306**, 666 (2004).
- Yu.A. Kurapov, L.A. Krushinskaya, V.V. Boretsky. Morphology of surface and fine structure of thick carbon films, produced by electron beam evaporations of carbon. *Electrometall. Today* **02**, 53 (2017).
- J. Robertson. Diamond-like amorphous carbon. *Mater. Sci. Eng. R* **37**, 129 (2002).
- L. Liu, M. Qing, Y. Wang, S. Chen. Defects in graphene: Generation, healing, and their effects on the properties of graphene: A review. *J. Mater. Sci. Technol.* **31**, 599 (2015).
- A.C. Ferrari, J. Robertson. Interpretation of Raman spectra of disordered and amorphous carbon. *Phys. Rev. B* **61**, 14095 (2000).
- niS.A. Konchits, B.D. Shanina, S.V. Krasnovyd, V.O. Yukhymchuk, O.M. Hreshchuk, M.Ya. Valakh, M.A. Skoryk, S.A. Kulinich, A.E. Belyaev, D.A. Iarmolenko. Structure and electronic properties of biomorphic carbon matrices and SiC ceramics prepared on their basis. *J. Appl. Phys.* **124**, 135703 (2018).
- L.G. Cancado, K. Takai, T. Enoki, M. Endo, Y. Kim, H. Mizusaki, A. Jorio, L. Coelho, R. Paniago, M.A. Pimenta. General equation for the determination of the crystallite size  $L[a]$  of nanographite by Raman spectroscopy. *Appl. Phys. Lett.* **88**, 163106 (2006).
- J. Etula, N. Wester, S. Sainio, T. Laurila, J. Koskinen. Characterization and electrochemical properties of iron-doped tetrahedral amorphous carbon (ta-C) thin films. *RSC Adv.* **8**, 26356 (2018).
- M. Rouhani, J. Hobley, F. Chau-Nan Hong, Yeau-Ren Jeng. In-situ thermal stability analysis of amorphous Si-doped carbon films. *Carbon* **184**, 772 (2021).

22. J. Vegh. The Shirley-equivalent electron inelastic scattering cross-section function. *Surface Science* **563**, 183 (2004).

Received 26.09.23.

Translated from Ukrainian by O.I. Voitenko

*В.О. Юхимчук, В.М. Джаган,  
О.Ф. Ісаєва, П.М. Литвин, А.А. Корчовий,  
Т.М. Сабов, В.Б. Лозінський, В.С. Єфанов,  
В.О. Осокін, Ю.А. Куратов*

СТРУКТУРНІ ТА МОРФОЛОГІЧНІ  
ВЛАСТИВОСТІ НАНОМЕТРОВИХ ВУГЛЕЦЕВИХ  
ПЛІВОК, ОТРИМАНИХ РОЗПИЛЕННЯМ  
ГРАФІТУ ЕЛЕКТРОННИМ ПРОМЕНЕМ

Методом електронного розпилення графіту отримано нанометрові вуглецеві плівки на металевих (мідних, сталевих) та кремнієвих підкладах. Температура підкладок варіювалася від 350 до 600 °С з кроком 50 °С, а час наплення – від 1 до 10 с. Отримані вуглецеві плівки характеризувалися методами раманівської спектроскопії, X-променевої фо-

тоелектронної спектроскопії (XPS), атомно-силової мікроскопії та електронного парамагнітного резонансу (EPR). З аналізу раманівських спектрів встановлено, що при температурах металевих підкладок до 400 °С, сформовані на них вуглецеві плівки є аморфними, при вищих температурах мають графітоподібну структуру. На кремнієвих підкладах при всіх температурах до 600 °С формуються аморфні вуглецеві плівки. Отримані результати з раманівських спектрів корелюють з даними XPS. Показано, що на морфологію плівок впливає як температура підкладок, так і їхній тип (металева чи кремнієва). Зі збільшенням температури підкладок від 350 до 600 °С середні розміри нерівностей на поверхні вуглецевих плівок зростають як на металевих, так і на кремнієвій підкладах. EPR дослідження показали, що наявні в плівках структурні дефекти, які зумовлюють прояв у раманівських спектрах так званих дефектних смуг ( $D$  та  $D'$ ), є не парамагнітними.

*Ключові слова:* вуглецеві аморфні плівки, графітоподібні плівки, раманівська спектроскопія, електронне розпилення, XPS, АСМ.